PERGAMON

International Journal of Heat and Mass Transfer 44 (2001) 2413–2422

International Journal of HEAT and MASS TRANSFER

www.elsevier.com/locate/ijhmt

Autoignition of sprays in a cylindrical combustor

Sang Hun Kang, Seung Wook Baek *, Ji Hun Choi

[a] *Department of Mechanical Engineering, Division of Aerospace Engineering, Korea Advanced Institute of Science and Technology, 373-1 Kusung-Dong, Yusung-Gu, Taejon 305-701, South Korea*

Received 3 March 2000; received in revised form 6 September 2000

Abstract

In this work, the physical characteristics of autoignition phenomena of liquid fuel sprays injected into hot and stagnant air, has been investigated. Eulerian (gas)/Lagrangian (droplets) formulations were adopted to analyze the two-phase flow in a confined 2D axisymmetric cylindrical combustor. The unsteady governing equations were solved considering two-phase interactions together with the particle source in cell (PSI-cell) model, which accounts for the finite rates of transports between phases. Instead, an infinite conduction model was adopted for the vaporization of droplets. The results have shown that the process of the autoignition is governed by droplet heating, vaporization, mixing and chemical reaction. The onset of ignition was determined by an incipience of the rapid increase in the maximum reaction rate. The effect of initial gas temperature on ignition delay time was found to be dominant, followed by the initial droplet size. However, it was also found that the injection angle as well as the injection velocity plays some role in affecting the ignition delays.

1. Introduction

Applications of spray combustion can be found in many practical systems such as diesel engine, gas turbine combustor, industrial furnace and so on. Spray combustion includes a number of complicated physical processes such as vaporization, mixing, ignition, combustion and radiative heat transfer. Among them, the ignition phenomenon is a crucial process, since it is an incipient process required for major heat release as well as one of deterministic factors for the system efficiency. For example, in diesel engine system, the autoignition under high-temperature and high-pressure conditions influences the whole performance of engine system. On the other hand, the autoignition phenomena in the delivery system of combustible mixture must be restricted to prevent a severe damage. Therefore, an understanding of the detailed physical and chemical processes, which govern an autoignition in spray combustion, is highly desired from a practical point of view. However, there are many difficulties in analyzing the problem of autoignition and spray combustion due to their inherently complicated thermo-fluid mechanical as well as chemical characteristics. Hence, most of researchers used to choose physically simple as well as reliable models. In order to successfully model the autoignition, following unsteady behaviors must be taken into account: spray injection, droplet heating, two-phase dynamics and interactions, phase change and chemical reactions.

In liquid fueled spray combustion, the fuel is injected into an environment of hot air as discrete droplet groups. Thus, the analysis must be extended to include two-phase coupling in the mass, momentum and energy equations. In this study, separated flow (SF) model [1] is used for detailed consideration of the finite rates of transports between phases. Ignition delay time, which is governed by various thermo-physical as well as chemical factors [2], is usually introduced to represent basic characteristics of autoignition, i.e., the rapid transition from non-reactive state to reactive state by a global heating of the mixture. Therefore, the parametric study of ignition delay is very important in fully understanding the autoignition process. Regarding this, a great deal of effort has been made to explain the autoignition

* Corresponding author. Tel.: +82-42-869-3714; fax: +82-42-869-3710.

E-mail address: swbaek@sorak.kaist.ac.kr (S.W. Baek).

0017-9310/01/$ - see front matter
PII: S0017-9310(00)00283-0

Nomenclature

A	Arrhenius factor ($m^3/mol/s$)
A_d	cross-section of droplet (m^2)
B	transfer number
C_d	drag coefficient of droplet
C_p	constant-pressure specific heat (J/kg/K)
d	droplet diameter (m)
D	diffusion coefficient (m^2/s)
dV_ϕ	control volume for variable ϕ (m^3)
E_a	activation energy (J/mol)
h	enthalpy (J/kg)
L	heat of vaporization (J/kg)
n	number of droplets in the characteristic group
Nu	Nusselt number
Pr	Prandtl number
R_f	reaction rate ($kmol/m^3/s$)
R'	universal gas constant ($=8.314$ J/mol/K)
Re	Reynolds number
S_ϕ	source term of variable ϕ
t	time (s)
T	temperature (K)
u	axial velocity (m/s)
v	radial velocity (m/s)
W	molecular weight (kg/kmol)
x	axial distance (m)
y	radial distance (m)
Y	mass fraction

Greek symbols

ϕ	dependent variable
μ	viscosity ($N\ s/m^2$)
Γ_ϕ	exchange coefficient
v	stoichiometric ratio
θ	injection angle, degree
ρ	density (kg/m^3)

Subscripts

c	CO_2
d	droplet (liquid)
f	fuel (gas)
g	gas phase
h	H_2O
i	species
o	oxidizer
s	droplet surface

phenomena. Experimental studies are performed in a variety of configurations and for a wide rage of conditions. However, there are no benchmark data available for standard conditions that can be used for validation of computational studies of the ignition phenomena [3]. Theoretical investigations have been done by adopting phenomenological models [4], transient one-dimensional models [5–7] and steady-state multidimensional models [8] with single-step or reduced multistep chemical mechanisms. However, the unsteady multidimensional simulation has yet to be investigated in further detail. Since the sprays experience many physical processes in a non-homogeneous condition, the one-dimensional model cannot represent various phenomena occurring in the real combustor. Also the determination of ignition delay by the distance between a nozzle tip and a flame front and the droplet history using steady-state model is inconclusive in exactly reproducing the transient variation of autoignition phenomena.

Based on these facts above, major objectives in this work are to represent and understand the processes of autoignition through more detailed modeling and to examine the effects of various injection conditions on the ignition phenomena by simulating a development of spray combustion in a confined cylindrical combustor. While the TEACH code is modified and used to solve the unsteady gas field with the PSI-cell model employed for finite transport rates between two phases and the infinite conduction model for the vaporization of droplets, the Lagrangian formulation is used to track the evolution of the droplets.

2. Formulations

The schematic for this study is presented in Fig. 1. Fuel droplets injected start to experience the heating up to boiling temperature by surrounding stagnant hot air. Once the droplet boiling temperature is reached, vaporization occurs and then its fuel vapor mixes with air and burns. In order to study the autoignition phenomena in a 2D axisymmetric combustor, the following assumptions are used: (1) unsteady and axisymmetric

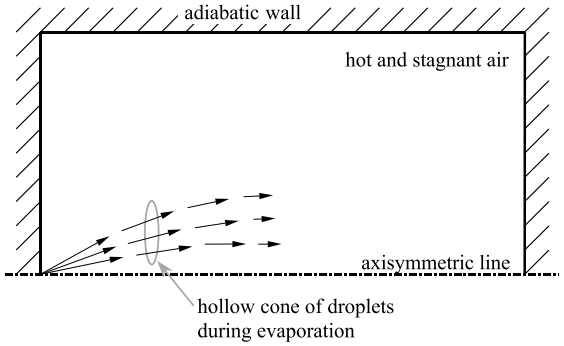

Fig. 1. Schematic of the axisymmetric combustor.

system, (2) negligible turbulence effect, (3) spherical droplets, (4) no interaction between droplets, (5) single reaction step with a second order, and (6) ideal gas. These physical processes can be represented by the following gas and droplet equations.

2.1. Gas field equations

The general governing equation for the gas field in axisymmetric coordinates is presented in Eq. (1), which is based on the Eulerian approach

$$\frac{\partial(\rho\phi)}{\partial t}+\frac{\partial}{\partial x}\left(\rho u\phi-\Gamma_\phi\frac{\partial\phi}{\partial x}\right)+\frac{1}{y}\frac{\partial}{\partial y}\left(y\rho v\phi-y\Gamma_\phi\frac{\partial\phi}{\partial y}\right)=S_{\phi,g}+S_{\phi,l}. \tag{1}$$

In this equation, ϕ, ρ, and Γ are the general dependent variable (mass, momentum, energy, species and etc.), density and diffusion coefficient. S_ϕ includes the source term of dependent variable for the gas and liquid phases and other terms which are transposed from the left-hand side of the equation. Specific representations of dependent variable are tabulated in Table 1.

2.2. Droplet equations

Since the existence of liquid droplets introduces droplet evaporation and mixing with air, an appropriate modeling that describes interactions between gas and liquid phases is required. In order to deal with this problem, the PSI-cell method [9] is adopted here in numerical procedure. With this model, droplet equations are cast in the Lagrangian form, coupled with the gas-phase field through the source terms ($S_{\phi,l}$). All droplets injected are arranged into a finite number of groups, each of which comprises a specified number of droplets. Droplet trajectory, velocity, temperature and droplet diameter could be traced by solving the following governing equations for droplets.

While following Eq. (2) is the mass conservation for the droplet as proposed by Faeth [1], the droplet evaporation rate in quasi steady state, $\dot{m}_{\text{sphere}}$ is empirically determined by Eq. (3) under the assumption of spherical shape.

$$\frac{\mathrm{d}m_\mathrm{d}}{\mathrm{d}t}=\dot{m}_{\text{sphere}}\left(1+0.3Re^{0.5}Pr^{0.33}\right), \tag{2}$$

$$\dot{m}_{\text{sphere}}=2\pi d\rho D\ln(1+B), \tag{3}$$

where D and B are the diffusion coefficient and Spalding's transport coefficient which is expressed by Eq. (4)

$$B=\frac{Y_{\text{fs}}-Y_\text{f}}{1-Y_\text{f}} \tag{4}$$

in which Y_{fs} is the fuel mass fraction on the droplet surface, which can be obtained from the Antoine's vapor

Table 1
Variables and source terms used in Eq. (1)

Equation	ϕ	Γ_ϕ	$S_{\phi,g}$	$dV_\phi S_{\phi,l}$
Continuity	1	0	0	$\sum \dot{m}\dot{n}$
Axial momentum	u	μ	$-\frac{\partial p}{\partial x}+\frac{\partial}{\partial x}\left(\mu\frac{\partial u}{\partial x}\right)+\frac{1}{y}\frac{\partial}{\partial y}\left(y\mu\frac{\partial v}{\partial x}\right)$	$\sum\left(\dot{m}\dot{n}u-\frac{4}{3}\pi\rho_\mathrm{d}r_\mathrm{d}^3\dot{n}F_\phi\right)$
Radial momentum	v	μ	$-\frac{\partial p}{\partial y}-\frac{2\mu v}{y^2}+\frac{\rho w^2}{y}+\frac{\partial}{\partial x}\left(\mu\frac{\partial u}{\partial y}\right)+\frac{1}{y}\frac{\partial}{\partial y}\left(y\mu\frac{\partial v}{\partial y}\right)$	$\sum\left(\dot{m}\dot{n}v-\frac{4}{3}\pi\rho_\mathrm{d}r_\mathrm{d}^3\dot{n}F_\phi\right)$
Energy	h	Γ	$\frac{\partial p}{\partial t}+\mu G+W_\mathrm{f}\dot{Q}R_\mathrm{f}$	$\sum\left\{-\dot{m}\dot{n}\left(C_\mathrm{p}\left(T_\mathrm{g}-T_\mathrm{d}\right)+L\right)\right\}$
Mass fraction (fuel)	Y_f	Γ	$-W_\mathrm{f}R_\mathrm{f}$	$\sum\dot{m}\dot{n}$
Mass fraction (other species)	Y_i	Γ	$\mp\nu_\mathrm{i}W_\mathrm{f}R_\mathrm{f}$ (− for O_2, + for product)	0

$$\Gamma=\frac{\mu}{\sigma_\phi},\ G=2\left[\left(\frac{\partial u}{\partial x}\right)^2+\left(\frac{\partial v}{\partial y}\right)^2+\left(\frac{v}{y}\right)^2\right]+\left(\frac{\partial u}{\partial y}+\frac{\partial v}{\partial x}\right)^2,\ F_\phi=\frac{\partial\phi_\mathrm{d}}{\partial t}$$

pressure equation [10]. Eq. (5) represents the momentum conservation equation for the droplet by considering the effects of drag force and pressure gradient

$$m_d\left(\frac{du_d}{dt}\right)=\frac{1}{2}\rho_g C_d(u-u_d)|u-u_d|A_d-\left(\frac{m_g}{\rho_g}\frac{\partial p}{\partial x}\right). \tag{5}$$

While droplet velocity can be calculated by integrating du_d/dt, its trajectory is followed by integrating the droplet velocity. Energy conservation equation is represented by Eq. (6), in which Nu is the Nusselt number set to $Nu=2+0.6Re^{0.5}Pr^{0.33}$ [1]

$$m_d\frac{dT_d}{dt}=\frac{Nu\pi kd}{C_{pd}}(T-T_d)-\frac{L}{C_{pd}}\dot{m}_d, \tag{6}$$

where the latent heat of vaporization, specific heat of the droplet and thermal conductivity of the gas are denoted by L, C_{pd}, and k. Finally, variation of droplet diameter can be traced using Eq. (7) with the mass flow rate determined by Eq. (2)

$$-\frac{d}{dt}\left(\frac{\rho_d\pi d^3}{6}\right)=\dot{m}_d. \tag{7}$$

2.3. Chemical reaction

The chemical reaction is assumed to be governed by a one step, second-order reaction with the Arrhenius form. The fuel and oxidizer used are *n*-decane and air. Its physical properties are shown in Table 2 [11,12]. The reaction rate is determined by the Arrhenius reaction rate, based on a one step reaction mechanism as given by Westbrook and Dryer [12]

$$R_f=A[\text{fuel}]^a[O_2]^b\exp\left[-\frac{E_a}{R'T}\right]. \tag{8}$$

3. Numerical algorithm

In order to solve the general governing equations for the gas field which is based on the Eulerian approach, the TEACH code [13], which had been used to modeling the spray combustion by Choi and Baek [14], is modified to account for the fully transient phenomena adopted in this study. Fig. 2 illustrates the computational flowchart for the solution procedure. First of all, the gas flow field is solved by using the modified TEACH code without an interaction with the liquid droplet. Given reasonably converged flow variables, PSIC subroutine is called to determine the trajectories and histories of the droplets as well as the coupling terms between two phases. And then, these coupling terms are substituted into the source terms in the gas-phase equations. Just a few iterations between flow solver and PSIC solver may be required. If all the solution is convergent, the time step for the flow field is increased and the upper procedure is repeated again.

Table 2
Fuel properties

Fuel	*n*-Decane ($C_{10}H_{22}$)
Molecular weight	142.3 kg/kmol
Heat of vaporization	3.619×10^5 J/kg
Boiling point	447.15 K
Specific heat	2200.8 J/kg/K
Density	733 kg/m^3
Activation energy	30 kcal/mol
Arrhenius factor	3.8×10^{11} cm^3/mol/s

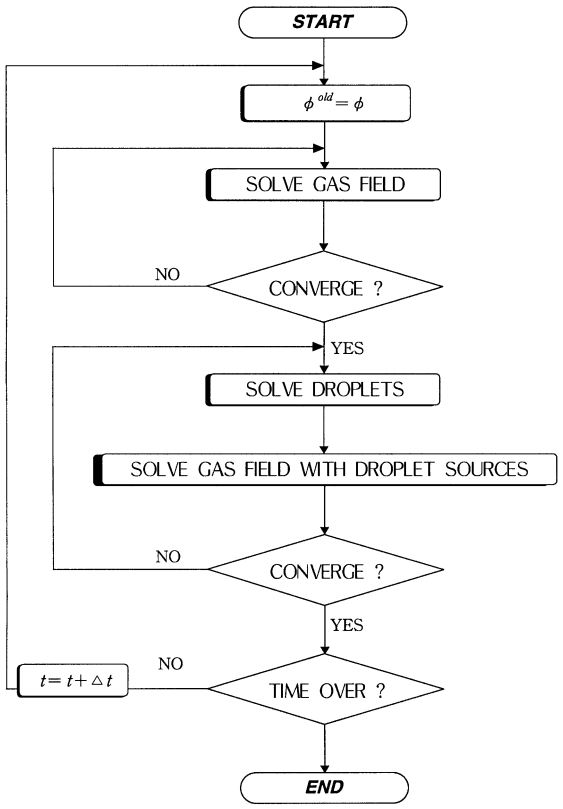

Fig. 2. Computational flowchart.

In order to check the effects of the time step on the calculation, a number of cases had been tried [15]. An appropriate value of time step for the gas field (Δt_g), the droplet trajectory (Δt_d) and the droplet injection (Δt_{inj}) were, respectively, determined within given convergence criteria after many preliminary calculations.

4. Results and discussion

The numerical simulation has been performed for non-premixed two-phase spray combustion in a confined

cylindrical combustor. Unless otherwise mentioned, the reference conditions are as follows: (1) combustor is 0.05 m radius and 0.1 m long, 2) the air in combustor is initially hot and stagnant (1000 K, 1 atm), (3) the fuel is *n*-decane, (4) the total injection time is 1 ms with fuel mass flow rate of 0.001 kg/s, (5) the droplet diameter is 100 μm and monodispersed, (6) initial velocities of all droplets are 15 m/s, (7) droplets are injected in 12

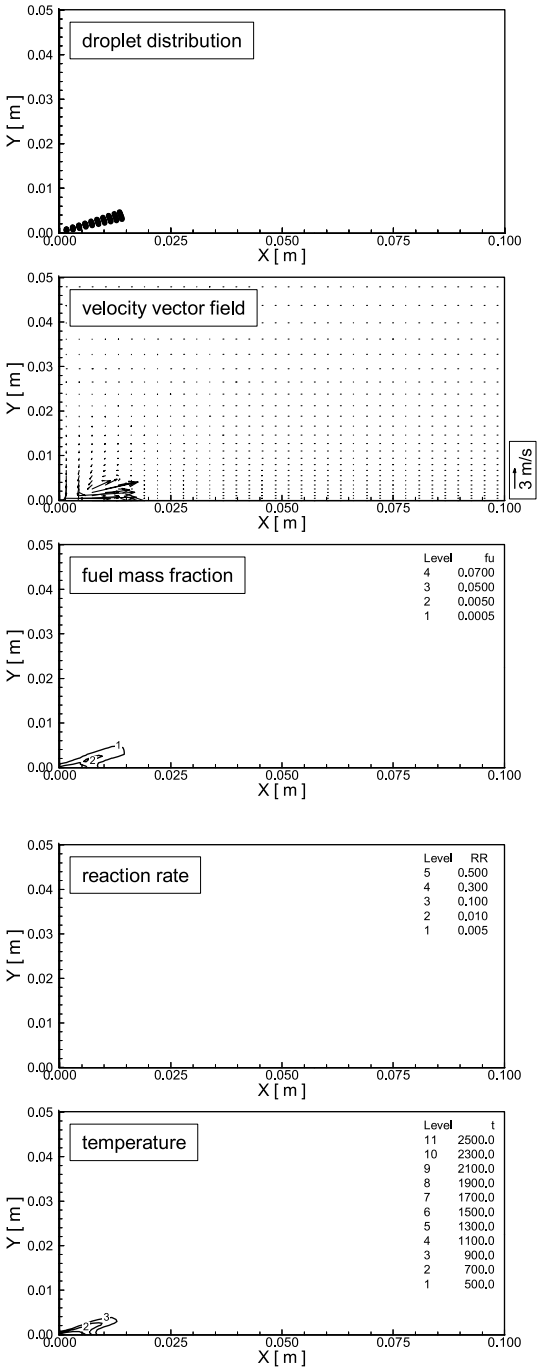

Fig. 3. Transient behaviors of droplet distribution, velocity field, fuel mass fraction, reaction rate and gas-phase temperature at 1.0 ms.

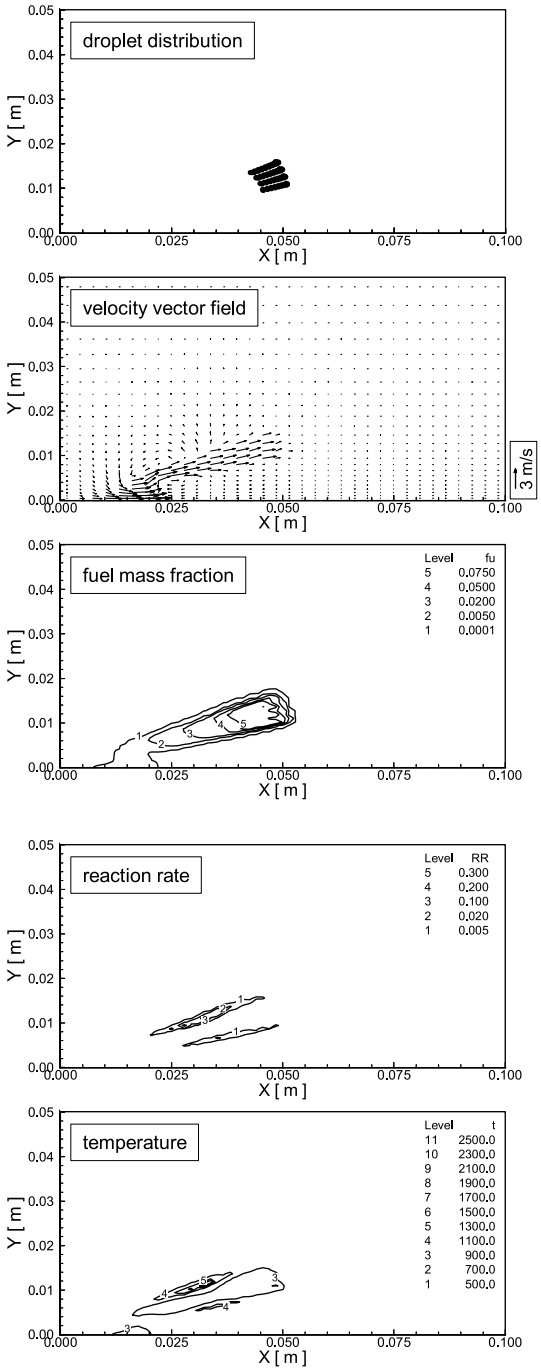

Fig. 4. Transient behaviors of droplet distribution, velocity field, fuel mass fraction, reaction rate and gas-phase temperature at 4.5 ms.

different directions (three different radial positions of $y = 0.10$, 0.25, and 0.40 mm with four different angles of $\theta = 12°,\ 14°,\ 16°$ and 18° at each position).

The processes of autoignition are presented in Figs. 3–6 for various times (1.0, 4.5, 5.0 and 10.0 ms). At 1.0 ms time level, the droplets are distributed near a nozzle and the heating up of droplets is in progress. Therefore, the induced flow and a decrease of temperature by droplets are found near a nozzle. Since most of the heat, which is transferred from gas field to droplet, is

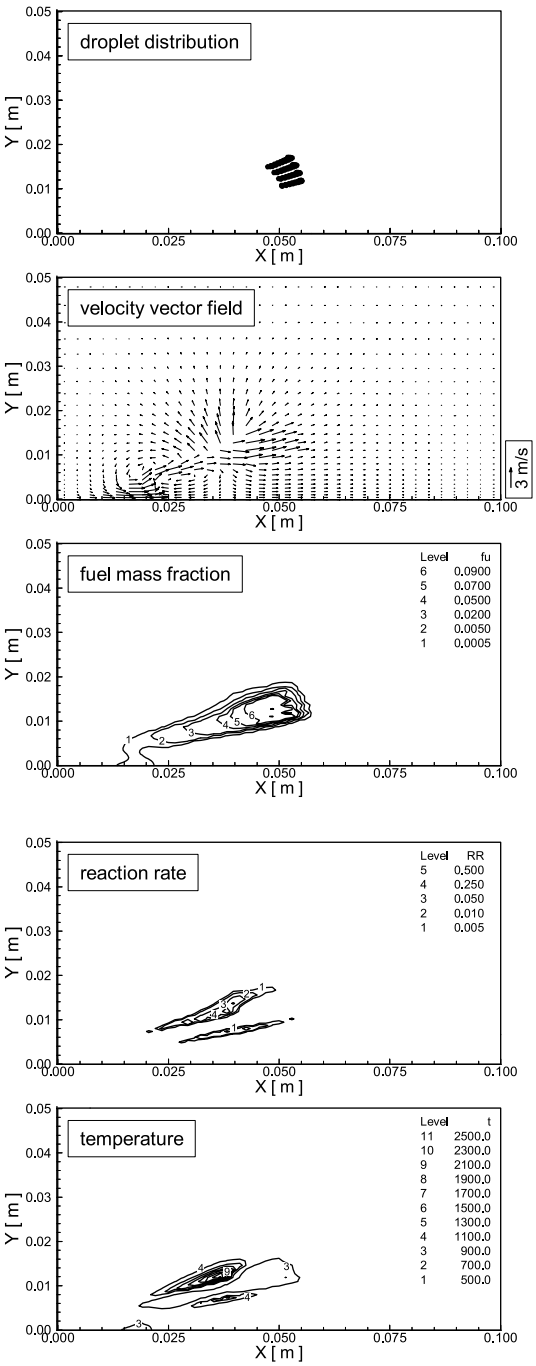

Fig. 5. Transient behaviors of droplet distribution, velocity field, fuel mass fraction, reaction rate and gas-phase temperature at 5.0 ms.

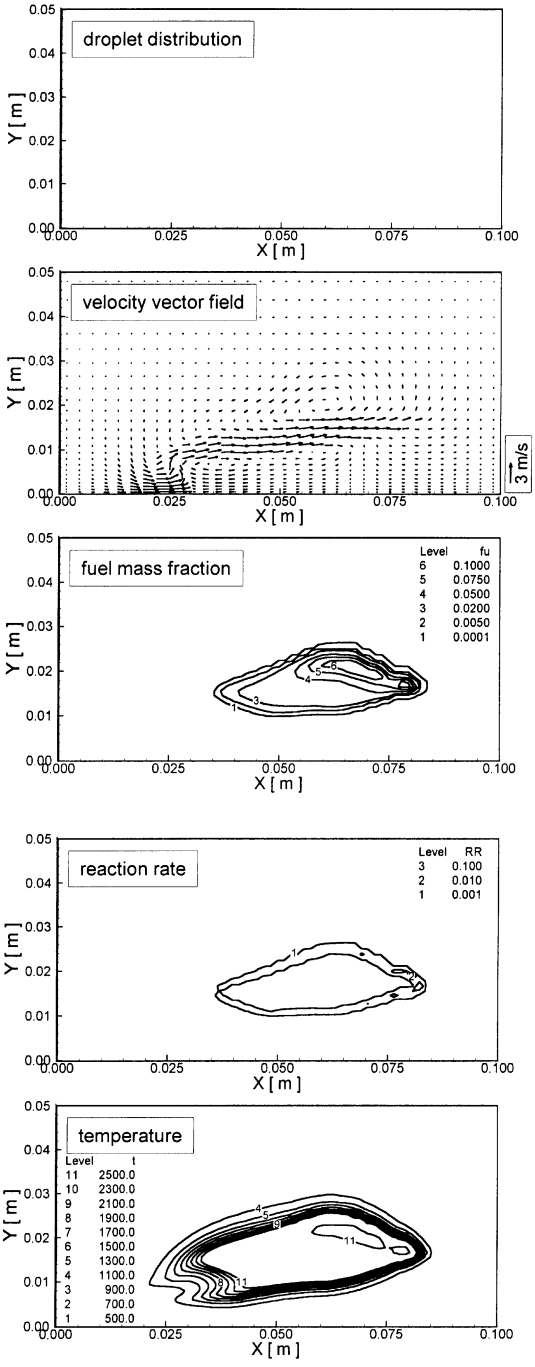

Fig. 6. Transient behaviors of droplet distribution, velocity field, fuel mass fraction, reaction rate and gas-phase temperature at 10.0 ms.

used to increase the droplet temperature, only a small amount of fuel is vaporized and the reaction is not found at this time. Fig. 4 shows the status at 4.5 ms after injection, when the ignition process is in progress. Before this time, the vaporization of liquid droplets and the mixing of gaseous fuel and air have simultaneously proceeded. The gas temperature in the vicinity of the droplets is seen to be still lower since the heat feedback from gas is used as the latent heat of liquid fuel. In the meantime, the gaseous fuel has been mixed with surrounding air, thereby forming a combustible mixture. The mixture is then heated by the surrounding hot air and finally the combustion must be initiated before 4.5 ms. The contours of reaction rate and fuel mass fraction show that the ignition kernel is placed along the droplet trajectory. Therefore, a high-temperature region is positioned along the high-reaction rate zone while a relatively low temperature region is located along droplet trajectory. At this time, the vaporization and mixing are observed to be still occurring.

At the time of 5.0 ms after fuel injection, the reaction becomes more intense so that its reaction zone is more broadly extended as shown in Fig. 5. At the time of 5.0 ms, a more heat transfer from the reaction zone must enhance the fuel vaporization and its reaction. The flame that is represented by large reaction rate in the figure is seen to be separated into two regions. The separated flames show that the spray combustion may not be described using a diffusion flame characteristic only [16]. The effect of gas expansion, which derives from the flame development, is obviously found in the velocity field. The high-temperature region gets continuously enlarged as the flame is developed. At 10.0 ms after fuel injection, the droplets have been totally evaporated so that they are not observed any more in Fig. 6. The reaction is more distributed around the gaseous fuel region and its rate is much reduced. Consequently, the high-temperature region is found to become broad.

Fig. 7 shows an unsteady variation of droplet temperature and droplet diameter squared. Depending on the injection position and angle, the droplets experience different thermal history. Except for an initial heating period and last burn-out period, all the variations of diameter squared (d^2) are seemingly linear. A discontinuous change in d^2 for each type of droplets after 6 ms is caused by a full development of gaseous flame. Among others, the droplets injected far from the symmetric axis, i.e., at larger y and θ undergo faster heating and thereby, faster decrease in d^2. This results from the fact that those droplets are less influenced by a reduction in the gas temperature due to heat transfer to the droplets than inner droplets.

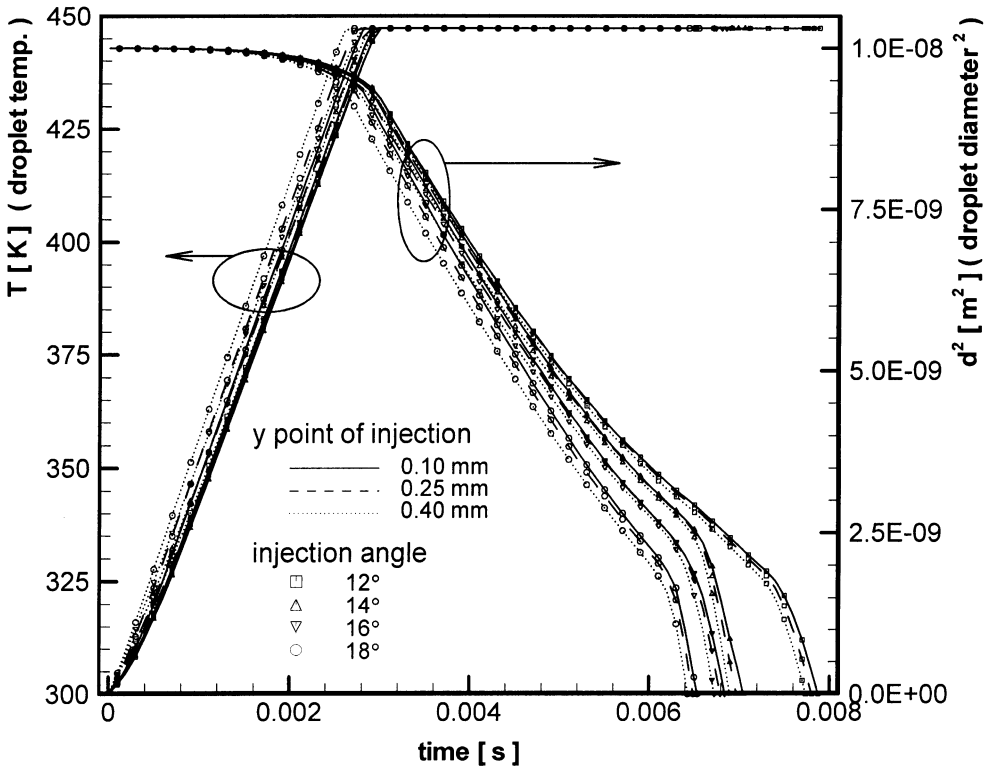

Fig. 7. Unsteady variation of droplet temperature and diameter squared.

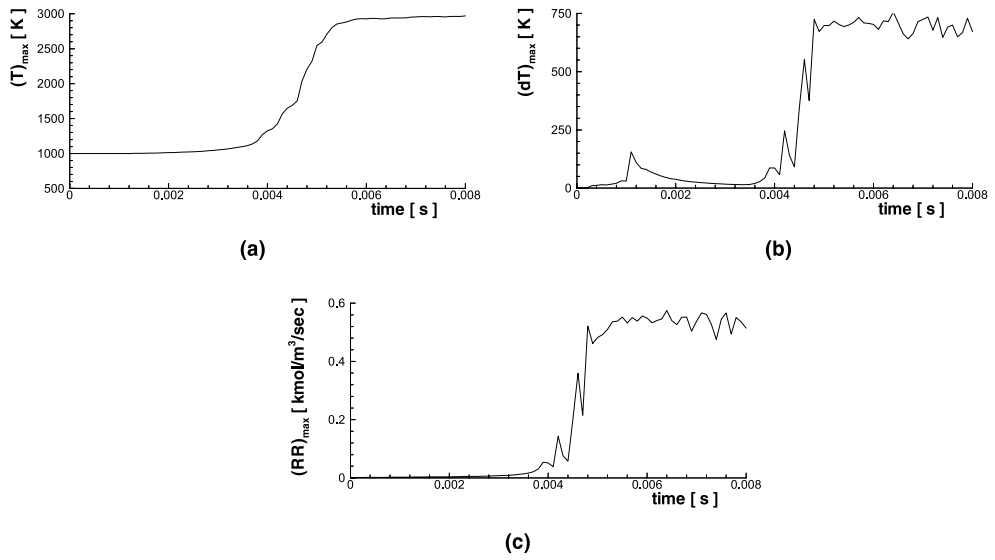

Fig. 8. Comparison of ignition criteria based on (a) maximum temperature; (b) maximum temperature differential; (c) maximum reaction rate.

The determination of ignition criteria is a very important and complicated problem for theoretical or computational investigation. In spite of various methods suggested by many researchers, there are no definite or universal criteria for ignition. Each researcher selects a specific one of various definitions, which is physically reliable for each investigation [3]. Therefore, the new ignition criterion must be also defined for this study. In Fig. 8, the unsteady changes of the maximum temperature, maximum variation of temperature and the maximum reaction rate in gas field are plotted. However, it must be noted that their maximum values do not always occur at the same position as time goes on. The figure shows that all values are closely related to each other so that their relation may be used to define the new ignition criterion to be used in the current numerical method. The maximum reaction rate and the maximum variation of temperature start to increase rapidly at about 4.2 ms. The maximum temperature is also seen to behave in a very similar manner. Before 4.2 ms, the liquid fuel undergoes evaporation while its vapor is being mixed with air, thereby forming the combustible mixture. A small peak of maximum variation of temperature at 1.0 ms represents the effect of termination of fuel injection. After the onset of ignition, the maximum reaction rate and maximum variation of temperature reach an approximately constant average value. Thus, the time at an incipience of the rapid increase in the maximum reaction rate is defined as an ignition delay time here.

There are also other parameters influencing the ignition delay; injection velocity, initial gas pressure and temperature, fuel type, droplet size and distribution in the chamber. The effect of the initial gas temperature on the ignition delay time is represented in Fig. 9. As expected, the ignition delay time rapidly decreases at low temperature zone while it slowly decreases in high-temperature zone as the initial gas temperature increases. The high-initial temperature field promotes a larger heat transfer from gas field to liquid phase. Hence, the time required for heating up of droplets and combustible mixture is shortened. Also the reaction rate, which is highly affected by the temperature and species mass fraction, becomes larger. Therefore, an increase in gas temperature decreases the ignition delay time.

The effect of the injection velocity on ignition is presented in Fig. 10. As shown in figure, when the injection velocity becomes larger, the ignition delay decreases. The relative velocity between two phases becomes larger as the injection velocity increases, since

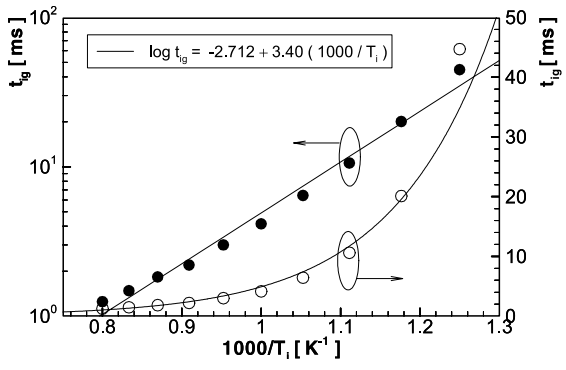

Fig. 9. Ignition delay against the inverse of initial gas temperature.

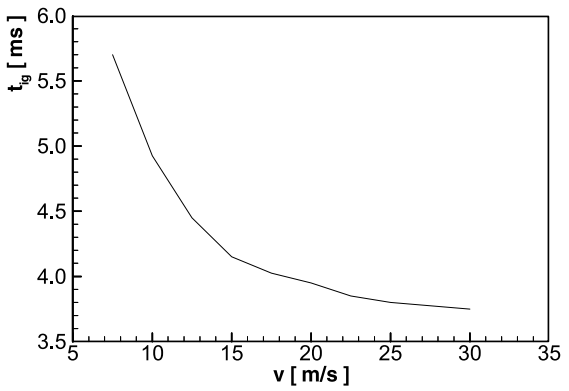

Fig. 10. The effect of injection velocity on the ignition delay (T_i = 1000 K, d = 100 μm).

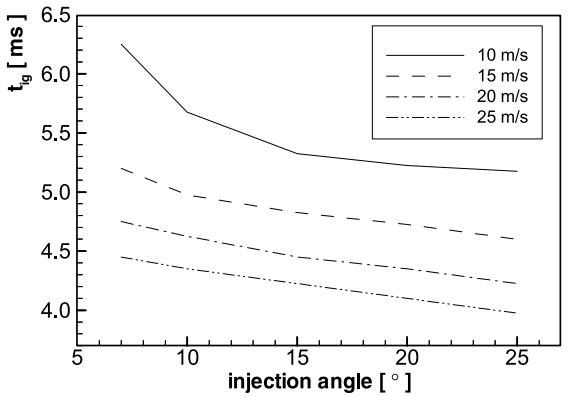

Fig. 12. The effect of droplet injection angle on the ignition delay for various injection velocities (T_i = 1000 K, d = 100 μm).

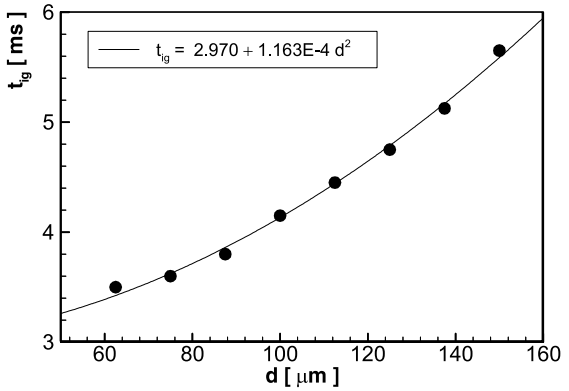

Fig. 11. The effect of droplet diameter on the ignition delay (T_i = 1000 K).

the droplets are injected into the stagnant air. Therefore, the increase in injection velocity enhances the heat exchange between droplet and gas so that the ignition delay time is reduced. In Fig. 11, the effect of the droplet diameter on the ignition delay time is presented when the total amount of fuel injected is fixed. When the droplet size becomes larger, the ignition delay steadily increases since the total evaporation rate is to be reduced because of smaller total surface area of droplets. Also the droplet distribution is another parameter that influences ignition. Fig. 12 shows the effects of droplet distribution on ignition when the injection angle is varied. In this case, the injection angles of droplets at three radial positions are all the same for a given injection angle in the figure. As the injection angle increases, the ignition delay time is shown to be shortened. This results from the fact that as the injection angle increases, the spatial volume the gas occupies increases due to its cylindrical geometry so that the particle number density is reduced. Consequently, this leads to the faster droplet vaporization since the decreasing rate of the gas temperature due to droplet heating slows down. However, the effect of number density is related to the conduction mode mainly. Thus, as the injection velocity, which is related to the convective heat transfer mode, increases, the effect of the injection angle becomes reduced as shown in Fig. 12.

5. Conclusion

In this study, an autoignition phenomenon of spray injection has been numerically investigated in a confined cylindrical combustor filled with hot and stagnant air, into which the liquid *n*-decane was injected. The process of spray combustion was numerically simulated by assigning injection location, injection angle and injection velocity. Typical physical characteristics of gas and droplets were temporally followed and discussed. The autoignition process comprises such several procedures as two-phase interaction, droplet heating, vaporization, mixing of gaseous fuel vapor and air and chemical reaction.

A premixed type of ignition kernel was observed on both the sides of fuel vapor zone along the droplet trajectory. The ignition criterion was numerically defined by comparison of temporal variations of the gas temperature and reaction rate. The rapid increase in the maximum reaction rate was regarded as the onset of ignition. The ignition delay time was estimated and discussed by changing such various parameters as initial gas temperature, initial droplet size and injection conditions. The effect of initial gas temperature was found to be the most significant while the effect of droplet size is relatively minor. However, in this study, it is also found that the injection angle as well as the injection velocity play some role in affecting the ignition delays.

References

[1] G.M. Faeth, Evaporation and combustion of spray, Prog. Energy Combust. Sci. 9 (1983) 1–76.
[2] K.K. Kuo, Principles of Combustion, Wiley, Singapore, 1986.
[3] S.K. Aggarwal, A review of spray ignition phenomena: present status and future research, Prog. Energy Combust. Sci. 24 (1998) 565–600.
[4] J. Sato, K. Konishi, H. Okada, T. Niioka, Ignition process of fuel spray injected into high pressure high temperature atmosphere, in: Proceedings of the 21st Symposium (International) on Combustion, 1986, pp. 695–702.
[5] S.K. Aggarwal, W.A. Sirignano, Ignition of fuel sprays: deterministic calculations for idealized droplet arrays, in: Proceedings of the 20th Symposium (International) on Combustion, 1984, pp. 1773–1780.
[6] E. Gutheil, Numerical analysis of the autoignition of methanol, ethanol, *n*-heptane and *n*-octane sprays with detailed chemistry, Combust. Sci. Technol. 105 (1995) 265–278.
[7] H.A. Dwyer, B.R. Sanders, Unsteady influences in droplet dynamics and combustion, Combust. Sci. Technol. 58 (1988) 253–265.
[8] B. Zuo, E. Van den Bulck, Fuel oil evaporation in swirling hot gas stream, Int. J. Heat Mass Transfer 41 (12) (1998) 1807–1820.
[9] C.T. Crowe, M.P. Sharma, D.E. Stock, The particle source in cell (PSI-cell) model for gas droplet flows, ASME J. Fluid Eng. (1977) 325–332.
[10] R.C. Reid, T.K. Sherwood, J.M. Pransnitz, The Properties of Gases and Liquids, McGraw-Hill, New York, 1987.
[11] T.E. Daubert, R.P. Danner, Physical and Thermodynamic Properties of Pure Chemicals, Hemisphere, New York, 1989.
[12] C.K. Westbrook, F.L. Dryer, Chemical kinetic modeling of hydrocarbon combustion, Prog. Energy Combust. Sci. 10 (1984) 1–57.
[13] A.D. Gosman, W.M. Pun, Lecture notes for course entitled calculation of recirculating flows, Imperial College of Science and Technology, London, Report No. HTS/74/2, 1973.
[14] C.E. Choi, S.W. Baek, Numerical analysis of a spray combustion with nongray radiation using weighted sum of gray gasses model, Combust. Sci. Technol. 115 (1996) 297–315.
[15] M.S. Raju, W.A. Sirignano, Spray combustion in a centerbody combustor, ASME J. Eng. Gas Turbines Pwr 111 (1989) 710–718.
[16] T. Kamimoto, H. Kobayashi, Combustion process in diesel engines, Prog. Energy Combust. Sci. 17 (1991) 163–189.